



Investigating sources of variability of monochromatic and transverse chromatic aberrations across eyes

Susana Marcos^{a,b,*}, Stephen A. Burns^a, Pedro M. Prieto^{a,c}, Rafael Navarro^b, Begoña Baraibar^b

^a Schepens Eye Research Institute, 20 Staniford Street, Boston, MA 02114, USA

^b Instituto de Optica 'Daza de Valdés', Consejo Superior de Investigaciones Científicas, Serrano 121, Madrid 28006, Spain

^c Laboratorio de Optica, Universidad de Murcia, Campus del Espinardo 30071 Murcia, Spain

Received 20 September 2000; received in revised form 26 January 2001

Abstract

Schematic eye models have typically been used to explain the average monochromatic and chromatic imaging properties of the eye. Both monochromatic aberrations and transverse chromatic aberration are known to vary widely across subjects. However, to our knowledge, the ability of schematic eye models to predict these individual variations has not been tested experimentally. We used a spatially resolved refractometer to measure the monochromatic aberrations and the optical transverse chromatic aberration (oTCA) in a group of 15 eyes. By recording the 1st and 4th Purkinje images for five directions of gaze, we also estimated the tilt, misalignment of ocular surfaces (front surface of the cornea and back surface of the lens) and off-axis position of the fovea (angle alpha), as well as pupil centration. We conclude that, contrary to expectations none of those factors are major contributors to the variability in monochromatic aberrations and oTCA in this group of eyes. Simulations show that corneal curvature and corneal conicity are also unlikely to account for the observed relation between monochromatic aberrations and oTCA. Our results suggest an important contribution of corneal irregularities to those aberrations. © 2001 Elsevier Science Ltd. All rights reserved.

Keywords: Angle alpha; Corneal aberrations; Human eye; Misalignment; Optical aberrations; Optical axis; Pupil; Purkinje images; Tilt; Transverse chromatic aberration; Wavefront

1. Introduction

In recent years there has been a growing interest in evaluating optical aberrations of the human eye, i.e. the optical imperfections inherent to the ocular optical system (Howland & Howland, 1977; Charman, 1991; Liang, Grimm, Goelz, & Bille, 1994; Navarro & Losada, 1997; He, Marcos, Webb, & Burns, 1998; Iglesias, Berrio, & Artal, 1998). This renewed interest has been partly stimulated by the awareness of the optical changes induced by refractive surgery (Applegate & Howland, 1997; Campbell, Haman, Simonet, & Brunette, 1999; Moreno-Barriuso, Merayo-Llaves, Marcos, Llorente, Navarro, & Barbero, 2001; Seiler, Kaemmerer, Mierdel, & Krinke, 2000) and by the

increased potential for compensation of the ocular aberrations to produce diffraction-limited optics (Liang, Williams, & Miller, 1997; Vargas-Martin, Prieto, & Artal, 1998; Zhu, Sun, Bartsch, Freeman, & Fainman, 1999; Navarro, Moreno-Barriuso, Bará, & Mancebo, 2000).

In normal eyes, the amount and pattern of monochromatic aberrations and the amount of transverse chromatic aberration (TCA, chromatic difference of position and magnification) vary widely across subjects (Howland & Howland, 1976; Ogbozo & Bedell, 1987; Simonet & Campbell, 1990; Thibos, Bradley, Still, Zhang, & Howarth, 1990; Rynders, Lidkea, Chisholm, & Thibos, 1995; Liang & Williams, 1997; He et al., 1998; Marcos, Burns, Moreno-Barriuso, & Navarro, 1999; Marcos & Burns, 2000;), while longitudinal chromatic aberration (chromatic difference of focus) varies little (Charman & Jennings, 1976; Howarth

* Corresponding author. Fax: +34-915645557.

E-mail address: susana@io.cfmac.csic.es (S. Marcos).

& Bradley, 1986; Rynders, Navarro, & Losada, 1998; Marcos et al., 1999).

A better insight into the sources of aberrations is critical to understand the relative contribution of cornea and lens to the overall image quality, to evaluate the outcomes for refractive surgery, in eye modeling, contact lens and intraocular lens design, and for ideal compensation of aberrations. Attempts to understand the causes of aberrations of the human eye, particularly chromatic aberration, have typically turned to the use of schematic eyes. The use of schematic eyes has the advantage that, by simplifying the optics to a limited number of surfaces of known shape, specific predictions can be made

Reduced single-surface eye models (Thibos, Ye, Zhang, & Bradley, 1992) typically attribute monochromatic aberrations such as coma (which is often referred to as the predominant source of image degradation, Howland & Howland, 1977) and TCA to pupil decentration and to the fact that the line of sight differs from the optical axis. More complex eye models account for some of the observed trends in optical performance (Lotmar, 1971; Navarro, Santamaría, & Bescós, 1985; Liou & Brennan, 1997; Escudero-Sanz & Navarro, 1999; Atchison & Smith, 2000b). However, schematic eye models are too generic to capture the true complexity of the aberrations in individual eyes.

In the current paper, we measure both monochromatic and chromatic aberrations in a set of eyes, together with major optical factors that eye models predict should have a major impact upon aberrations. We measured the tilt and misalignment of the ocular surfaces and pupil centration using the Purkinje images (Tscherning, 1924; Le Grand & El Hage, 1980). We then used a correlation approach to test whether the measured parameters can account for the actual variations in optical quality.

2. Methods

2.1. Subjects

We measured 15 eyes from nine normal subjects (seven men and two women, aged 25–50, mean 34). Spherical refraction ranged from 0 to -7 D, and astigmatism from 0 to 1.5 D. Monochromatic wave aberration, optical transverse chromatic aberration and Purkinje images were measured for one eye in a single session. All measurements except for one eye (with the pupil dilated with tropicamide 0.5%) were done under natural viewing conditions. A typical session lasted less than 1 h. An informed consent was obtained from all subjects participating in the study.

2.2. Measurement of ocular monochromatic aberrations

The monochromatic wave aberration was measured by means of a spatially resolved refractometer. This psychophysical technique, as well as the experimental procedure, has been described in detail elsewhere (Webb, Penney, & Thompson, 1992; He et al., 1998; He, Burns, & Marcos, 2000; Marcos et al., 1999; Burns & Marcos, 2001). The subject's task is to align, by means of a joystick, a test spot (which enters the pupil of the eye sequentially at 37 locations) to a cross, viewed through the pupil center. Both the test and the reference target were green. The pupil center was used as the reference and aligned to the optical axis of the instrument, using an IR video camera, which continuously monitors the pupil position). Since all measurements were done foveally, this operation aligned the line of sight to the optical axis of the instrument. The spherical refraction is corrected by means of a Badal system. The tilt necessary for the alignment at each point in the pupil is proportional to the slope of the ocular wave aberration at that pupil entry location. A session consists of three runs with 37 tilt settings. The wave aberration is estimated using a least-square fit of these tilts to the derivatives of a Zernike polynomial expansion up to the 7th order (35 terms). We used the root-mean-square (RMS) wavefront error as an image quality metric. We computed RMS (for all terms or specific orders) by adding the square of the Zernike coefficients (using the standard notation, Thibos, Applegate, Schwiegerling, Webb, & Members, 2000). All computations were done for a 7.32 mm pupil diameter.¹ For all computations, tilts and defocus have been cancelled. The Stiles–Crawford effect was not taken into account.

2.3. Measurement of optical transverse chromatic aberration

The spatially resolved refractometer can be used, as described by Marcos et al. (1999), to measure transverse chromatic aberration (both optical and perceived). In the present paper, we will consider only the optical transverse chromatic aberration (oTCA), i.e. the chromatic difference of position between a red and a blue target viewed through a small centered pupil. For this experiment, we substituted the green filter by a magenta filter, which produced a red and a blue spot (with peak wavelengths at 473 and 601 nm) when

¹ This diameter represents the furthest position within the system from which a light ray can enter the eye. However, in practice, while the subject needed to have a pupil of at least 6 mm, there were cases where it did not exceed 7 mm. We have tested that this difference between the actual pupil size and that used in computations does not affect the final data (He et al., 2000).

viewed through a pupil location away from the foveal achromatic axis. The subject's task was to align either the blue spot or the red spot to the center of the cross target, for the centered pupil position. Each experimental session consisted of six measurements: three using the blue spot and three using the red spot. The angular difference between the blue and the red settings is taken as the oTCA.

2.4. Measurement of alignment and centration of ocular components

We built a system to record the 1st (reflection from the front surface of the cornea) and 4th (reflection from the back surface of the crystalline lens) Purkinje images of the eye (Cornsweet & Crane, 1973; Barry, Effert, Kaupp, & Burhoff, 1994). A collimated 594 nm He–Ne laser beam illuminated the entire eye's pupil, while the subject viewed a target conjugate to the retina (brought into focus by a Badal system). The retinal fixation target consisted of five small circular apertures, one foveal and four at the corners of a square centered at the fovea and with 10 deg sides parallel to the horizontal and vertical axis, respectively. The fixation target was back-illuminated by a diffused 633 nm He–Ne laser. A high-resolution CCD camera collected the light reflected from the eye in a plane conjugate to the pupil. An IR-CCD camera monitored the pupil to ensure proper alignment. The light levels were all more than an order of magnitude below safety limits. We collected five pupil images, corresponding to foveal fixation, and to the four eccentric directions of gaze. From the location of the 1st and the 4th Purkinje image, we computed angle alpha and the pupil intersect of the optical axis with respect to the pupil center. We call angle alpha the angle formed by line of sight and the line passing through the centers of curvature of the front surface of the cornea and the back surface of the lens (Atchison & Smith, 2000a). The line passing through the centers of curvature of the front surface of the cornea and the back surface of the lens is an approximation of the optical axis (Le Grand & El Hage, 1980). Angle alpha provides a measurement of the tilt and misalignment of the front surface of the cornea and the back surface of the lens, including the effect of the separation of the fovea from the optical axis (Phillips, Perez-Emmanuelli, Rosskoth, & Koester, 1988; Dunne, Barry, Hartman, Culpin, de Main, & French, 1995). Fig. 1(a) shows images for a particular subject's right eye (S3-R), corresponding to five directions of gaze. The brightest image corresponds to the 1st Purkinje image, and the smaller, dimmer image to the 4th Purkinje image. Fig. 1(b) shows the procedure for estimating angle alpha, as the interpolation of the direction of gaze (visual angle) that will cause an overlapping of the 1st and 4th Purkinje images. The plot illustrates the determination of the horizontal and vertical coordinates of angle alpha, for the subject shown in Fig. 1(a). Filled circles represent the horizontal distance between the 1st and 4th Purkinje images and open circles the vertical distance. Solid lines represent linear fits to the data.

The pupil center is computed by fitting a circle to the margins of the pupil. The pupil position where the optical axis intersects the pupil lies along the line

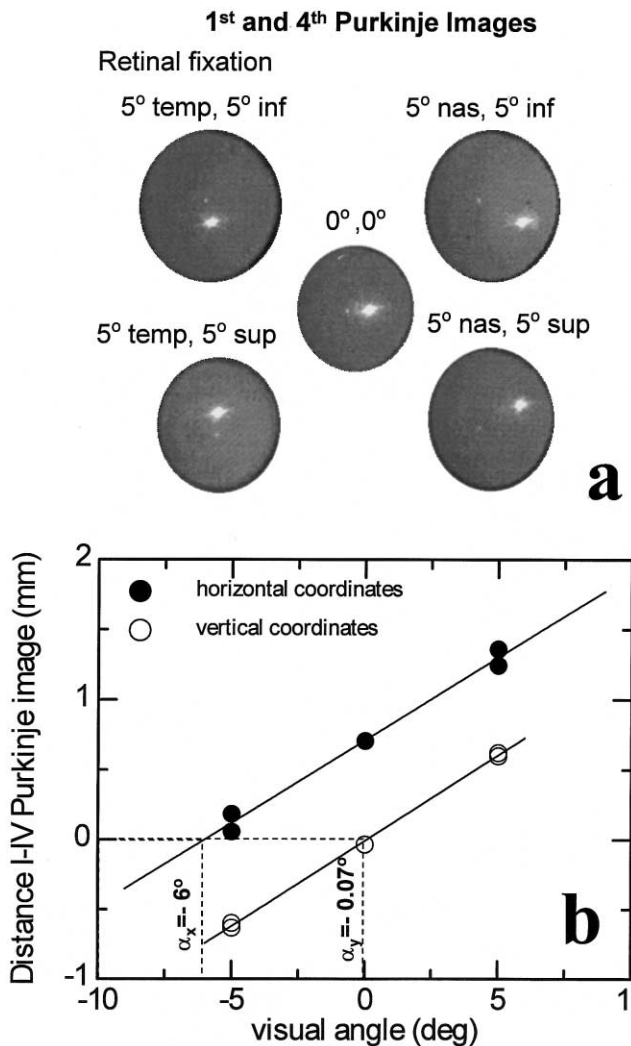


Fig. 1. Example of 1st and 4th Purkinje images recording (a) and estimation of angle alpha (b) for subject S3's right eye (S3-R). Images for five different directions of gaze are shown. The images are arranged as the corresponding retinal fixation targets. The bright spots correspond to the 1st Purkinje images, the dim spots to 4th Purkinje images. (b) Angle alpha is obtained by interpolation from the relative positions of the 1st and 4th Purkinje images as a function of visual angle, as the direction of gaze for which the 1st and 4th Purkinje image will overlap. Solid circles represent horizontal coordinates, and open circles represent vertical coordinates. The solid lines are best fits to the experimental data. The horizontal and vertical components of angle alpha for this subject are shown.

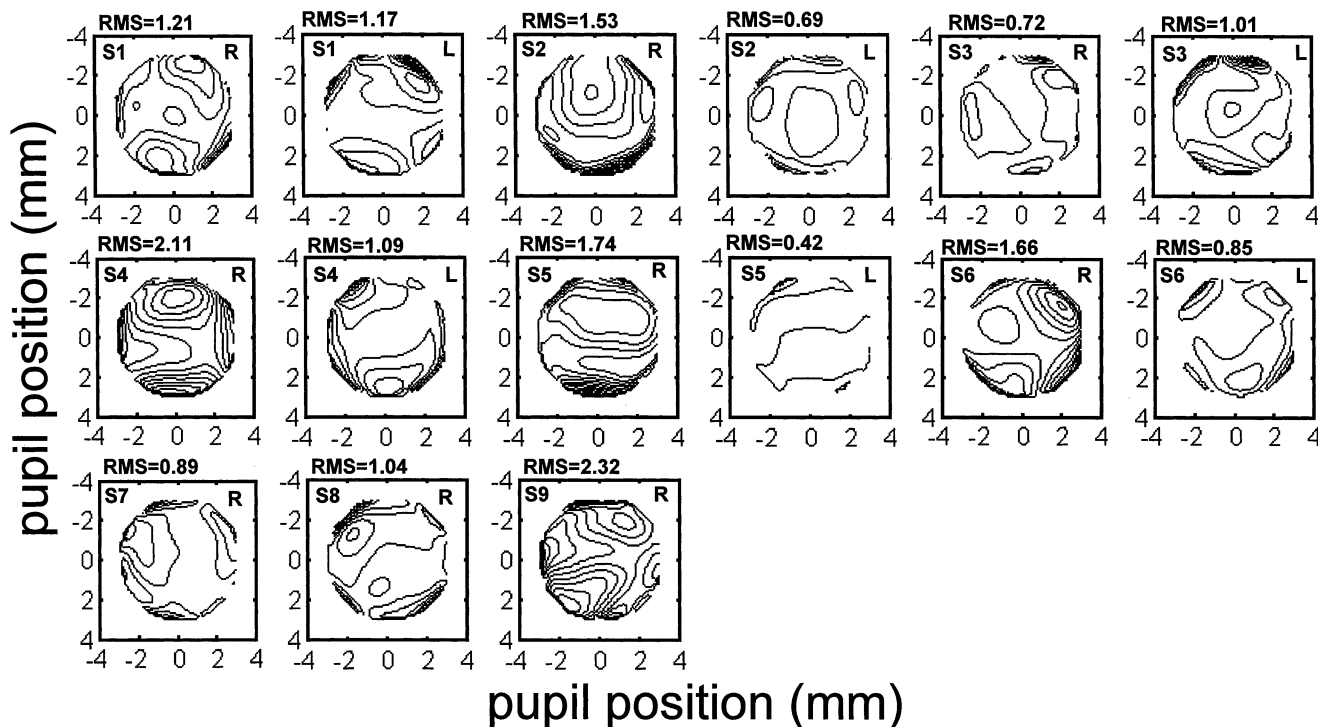


Fig. 2. Contour plots of the wave aberration maps (up to 7th order Zernike polynomials) for all 15 eyes in this study. Tilts and defocus were set to zero. R stands for right eyes, and L stands for left eyes. Adjacent R and L plots correspond to right and left eyes of the same subject. Positive horizontal coordinates stand for nasal pupil coordinates for right eyes and temporal for left eyes, and vice versa for negative horizontal coordinates. Positive vertical coordinates stand for superior pupil coordinates and negative for inferior, for both left and right eye. The contour line spacing is 1 μm . The corresponding root-mean-square (RMS) wavefront errors are given for each eye (in μm).

passing through the 1st and 4th Purkinje images (for foveal fixation). The distance from the 1st Purkinje image is proportional to the relative average separation of the 1st Purkinje images (related to corneal curvature) for the eccentric directions of gaze.

3. Results

3.1. Ocular monochromatic aberrations

Fig. 2 shows contour plots of the wave aberration for the 15 eyes measured in this study. R stands for right eye and L for left eye. Both eyes of the same subject have been plotted consecutively. Negative horizontal coordinates stand for temporal pupil position in right eyes and nasal for left eyes, and vice versa for positive horizontal coordinates. Negative vertical coordinates indicate inferior pupil locations, and positive superior pupil locations. Each map is the average of three experimental runs. The corresponding RMS wavefront error, including astigmatism and 3rd through 7th order terms are shown. There is significant intersubject variability (He et al., 1998) in both the distribution and amount of the aberrations in human eyes. There is also significant variability between left and right eye of the

same subject (Marcos & Burns, 2000). Mean standard deviations of Zernike coefficients (as defined by standardization committee, Thibos et al., 2000) are $0.075 \pm 0.024 \mu\text{m}$ across terms and subjects, and the mean standard deviations for the RMS is $0.093 \pm 0.07 \mu\text{m}$.

3.2. Optical transverse chromatic aberration

Fig. 3 shows horizontal and vertical coordinates of the optical transverse chromatic aberration (oTCA) for the 15 eyes. Filled symbols represent right eyes, open symbols represent left eyes. Labels next to the symbols refer the subject number. For both left and right eyes, the horizontal component of the oTCA is positive when the blue spot appears to the subject to lie to the left of the red spot, and vice versa. This convention matches (Thibos et al., 1990) for the left eye, and is the opposite for the right eye. For both eyes, the vertical component of the TCA is positive when the blue spot is below the red spot, and vice versa. Five of the 15 eyes exceeded 2 arcmin for total oTCA. Results from two of the subjects (S4 and S5) were reported in a previous paper (Marcos et al., 1999), where the effect of their aberrations and their own Stiles–Crawford effect on the perceived transverse chromatic aberrations were also studied. Incidentally, these subjects show the largest

differences in oTCA between left and right eyes. Standard deviations of the measurements ranged between 0.30 and 1.2 arcmin. We did not find a larger variability for those subjects exhibiting higher oTCA.

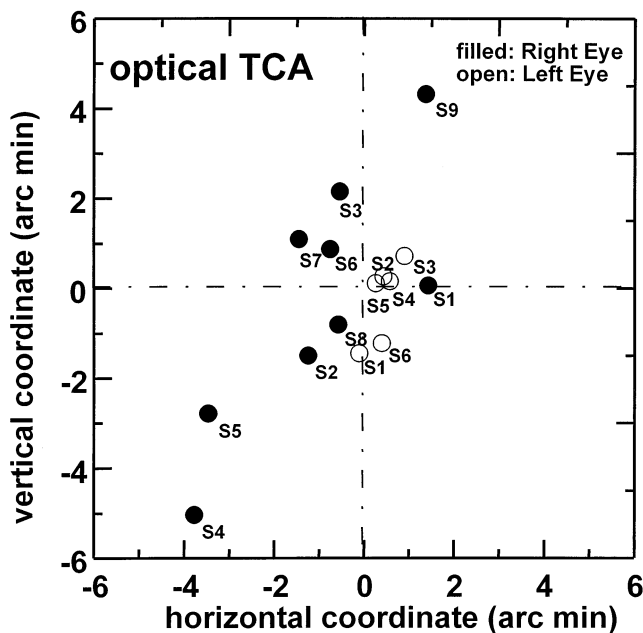


Fig. 3. Optical transverse chromatic aberration (oTCA)—horizontal versus vertical coordinates—for all 15 eyes. Solid circles represent right eyes and open circles represent left eyes. Labels refer to the subject number. For both left and right eyes, the horizontal component of the oTCA is positive when the blue spot appears to the subject to lie to the left of the red spot, and vice versa. For both eyes, the vertical component of the TCA is positive when the blue spot is below the red spot, and vice versa.

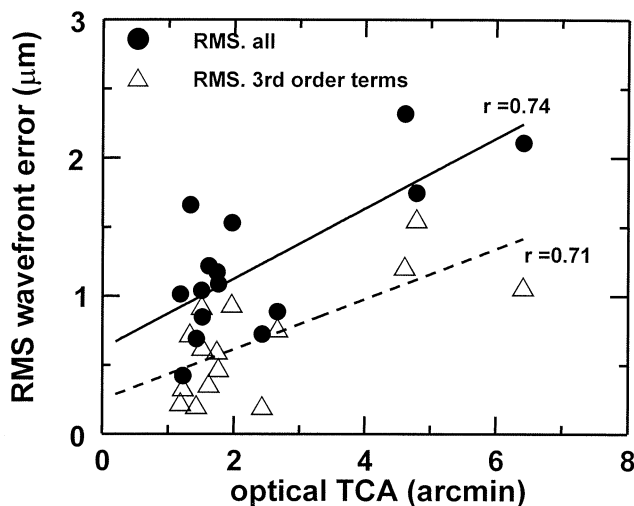


Fig. 4. Relationship between root-mean square wavefront error (RMS) and optical transverse chromatic aberration oTCA, including all terms in the Zernike polynomial expansion except for tilts and defocus (solid circles) and only 3rd order terms (open triangles). Lines represent linear fit to the data.

3.3. Relationship between ocular aberrations and optical transverse chromatic aberration

Large RMS values for monochromatic aberrations were associated with increased oTCA. Fig. 4 shows the relationship between RMS and oTCA. Filled circles represent RMS including all terms (except for tilt and defocus—the same result was found after canceling astigmatism as well), and open triangles represent RMS for 3rd order aberrations only (which includes coma terms). The lines represent linear regressions to the data. The correlation is statistically significant for both cases ($r = 0.74$, $P = 0.0009$ and $r = 0.71$, $P = 0.0021$, respectively).

3.4. Tilt and misalignment of ocular surfaces and pupil centration

Fig. 5(a) shows the horizontal and vertical coordinates of angle alpha (as defined and interpreted in the previous section) for all 15 eyes. Filled circles represent right eyes, and open circles represent left eyes. Labels next to the symbols refer to the subject number. In our convention, angle alpha is negative for right eyes and positive for left eyes, if the fovea is on the nasal side of the optical axis (as is typical). For both right and left eyes, angle alpha is positive if the fovea is superior with respect to the optical axis, and negative if the fovea is inferior relative to the optical axis. In this group of eyes, the total angle alpha ranged from 1.8 to 7.4 deg. Angle alpha is mirror symmetric between right and left eyes. The coefficient of correlation for the horizontal coordinates (significantly different from zero) is $r = 0.85$. Standard deviations of the measurements ranged between 0.15 and 0.92 deg.

Fig. 5(b) shows the positions of the 1st (circle), 4th (triangle) with respect to the pupil center, and estimated pupil intersect of the optical axis (cross) for all eyes, for foveal fixation. Filled symbols indicate right eyes, and open symbols indicate left eyes. Horizontal coordinates are positive for nasal decentration in right eyes and for temporal in left eyes, and are negative for temporal in right eyes and for nasal in left eyes. Positive stands for superior and negative for inferior decentrations for both right and left eyes. The separation of the optical axis from the pupil center is a measure of pupil centration and ranged from 0.05 to 0.40 mm. Correlations of the position of the Purkinje images and optical axis relative to the pupil center between right and left eyes indicate that pupil centration is bilaterally mirror symmetric: $r = 0.96$, $P = 0.0006$ for the 1st Purkinje image location, $r = 0.78$, $P = 0.06$ for the 4th Purkinje image location, and $r = 0.90$, $P = 0.03$ for the optical axis. In terms of reproducibility (across sessions) standard deviations ranged between 0.005 and 0.08 mm for the position of the 1st Purkinje Image, 0.02 and 0.10 for the

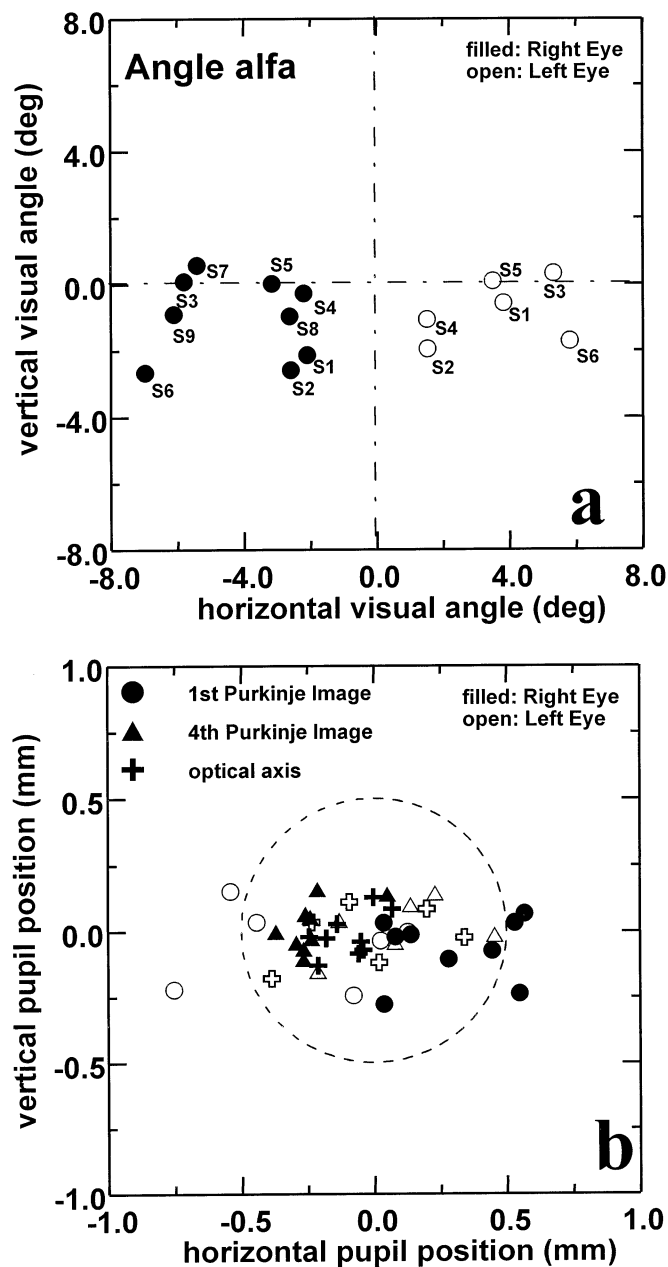


Fig. 5. (a) Angle alpha (horizontal versus vertical coordinates) for all 15 eyes. Filled circles represent right eyes, and open circles represent left eyes. Angle alpha is negative for right eyes and positive for left eyes, if the fovea is on the nasal side of the optical axis. Labels refer to the subject number. For both right and left eyes, angle alpha is positive if the fovea is superior with respect to the optical axis, and negative if the fovea is inferior relative to the optical axis. (b) Relative position (horizontal and vertical coordinates) of 1st Purkinje image (circles), 4th Purkinje image (triangles), and optical axis (crosses) with respect to the center of the pupil, for foveal fixation. The dotted circle represents a 0.5 mm radius pupil. Filled symbols indicate right eyes and open symbols indicate left eyes. Horizontal coordinates are positive for nasal decentration in right eyes and for temporal in left eyes, and negative for temporal in right eyes and for nasal in left eyes. Positive stands for superior and negative for inferior decentrations for both right and left eyes.

position of the 4th Purkinje image and 0.006 and 0.10 for the optical axis.

3.5. Control experiment

It has been shown that the pupil shifts slightly (± 0.2 mm on average) with dilation (Walsh, 1988; Wilson, Campbell, & Simonet, 1992). All our measurements were performed relative to the pupil center, and with comparable pupil sizes. Particularly, the pupil position of the optical axis and the optical transverse chromatic aberration (which is measured at the pupil center) rely on a proper and fixed pupil centration.

Our wave aberration measurements require a pupil diameter of at least 6 mm. Optical transverse chromatic aberration measurements were performed in the same system (the SRR) with pupil diameters also close to 6 mm. The average pupil diameter (across subjects and sessions) during the Purkinje measurement was 5.2 ± 1.7 mm. These differences are too small to account for any discrepancy due to pupil center shifts.

As a control experiment, we performed two Purkinje sessions, one on an eye with a pharmacologically dilated pupil (pupil diameter = 9.98 ± 0.16 mm), and the other on the same eye under natural viewing conditions (pupil diameter = 3.2 ± 0.12 mm). The differences in the pupil positions of the 1st, 4th and optical axis (which should not move with pupil size) were 0.30, 0.014 and 0.18 mm, respectively, only slightly above the standard deviations across measurements in the same conditions.

4. Discussion

We found large differences in the amount of monochromatic aberrations and optical transverse chromatic aberrations between eyes. Interestingly, eyes with higher amount of monochromatic aberrations also had higher amounts of oTCA. In the next Sections we use this measured variation in aberrations to test hypotheses that arise from the schematic eye models. Tests for hypotheses 1 and 2 address the predictions of most eye models that variations in angle alpha and pupil centration could be major contributors to individual variations in aberrations. Hypothesis 3 and 4 use more complete eye models to test whether incorporation of individual specific features of the tested eyes could improve the ability to predict individual variations.

4.1. Hypothesis 1: angle alpha

Tilt and misalignment of optical surfaces or a larger displacement of the fovea from the optical axis could give rise to both an increase in monochromatic aberrations

tions (particularly astigmatism and coma) and an increase in optical transverse chromatic aberration (Van Meeteren, 1974; Van Meeteren & Dunnewold, 1983; Atchison & Smith, 2000b). For a simple optical eye model, the larger the angle alpha, the larger the displacement of the visual axis (passing through the fovea and the nodal point) from the center of the pupil, and therefore the higher the amount of oTCA at the pupil center (Bennett & Rabbetts, 1984; Thibos, 1987). In this type of model, this displacement of the fovea is the primary source of oTCA, and increasing displacements are also expected to increase the wavefront error due to off-axis aberrations. Predictions based on this model are compatible with some of the observed values of oTCA found in the literature (Simonet & Campbell, 1990; Thibos et al., 1990) and with realistic values of

coma (van Meeteren & Dunnewold, 1983). However, those predictions were based on assumed average values of angle alpha. Fig. 6(a) shows the direct test of this relation. RMS wavefront error (for all terms except tilts and defocus in solid circles and for 3rd order terms in solid triangles) is plotted as a function of total angle alpha (computed as the modulus, from the vertical and horizontal components shown in Fig. 3), for all 15 eyes. There was no statistically significant correlation and little evidence of a possible trend. We can conclude that differences in the off-axis position of the fovea, tilt, misalignment and decentration of the cornea with respect to the lens (at least the front surface of the cornea with respect to the back surface of the lens) are not the main sources of individual variations in monochromatic aberrations in these eyes. Similarly, we did not find any correlation between angle alpha and oTCA (Fig. 6b).

Further support for the fact that angle alpha does not account for the variability found in monochromatic aberrations and oTCA is given by the analysis of bilateral symmetry in these subjects. Whereas angle alpha is symmetric between left and right eyes (indicating that the fovea is symmetrically located in left and right eyes, and that if tilts and misalignments happen between ocular surfaces they develop symmetrically between eyes), we do not find a corresponding symmetry of ocular aberrations and oTCA in this group of eyes. There must be other major sources of aberrations that are not necessarily as bilaterally symmetric.

4.2. Hypothesis 2: pupil centration

Pupil decentration is known to degrade retinal image quality (Van Meeteren & Dunnewold, 1983; Artal, Marcos, Iglesias, & Green, 1996), due to both an increase in the monochromatic aberrations (Van Meeteren & Dunnewold, 1983; Walsh & Charman, 1988) and an increase in transverse chromatic aberration (Thibos, 1987; Thibos et al., 1990; Bradley, Thibos, Zhang, & Ye, 1991; Artal et al., 1996).

Simple eye models, based on on-axis, rotationally symmetric components predict that coma (and consequently higher RMS wavefront error) will be produced if the pupil is decentered (Atchison & Smith, 2000b). In addition, pupil centration is a critical parameter in reduced eye models that allow them to predict optical transverse chromatic aberration. If the pupil is centered on the foveal achromatic axis, these models predict zero oTCA, whereas if the pupil is shifted from the foveal achromatic axis, oTCA will be proportional to the shift (Thibos et al., 1990).

We measured pupil centration relative to fixed positions on the pupil (1st and 4th Purkinje images for foveal fixation, and the pupil intersect of the optical axis), and correlated those distances with RMS [Fig. 7(a)] and oTCA [Fig. 7(b)]. In both figures, the distance

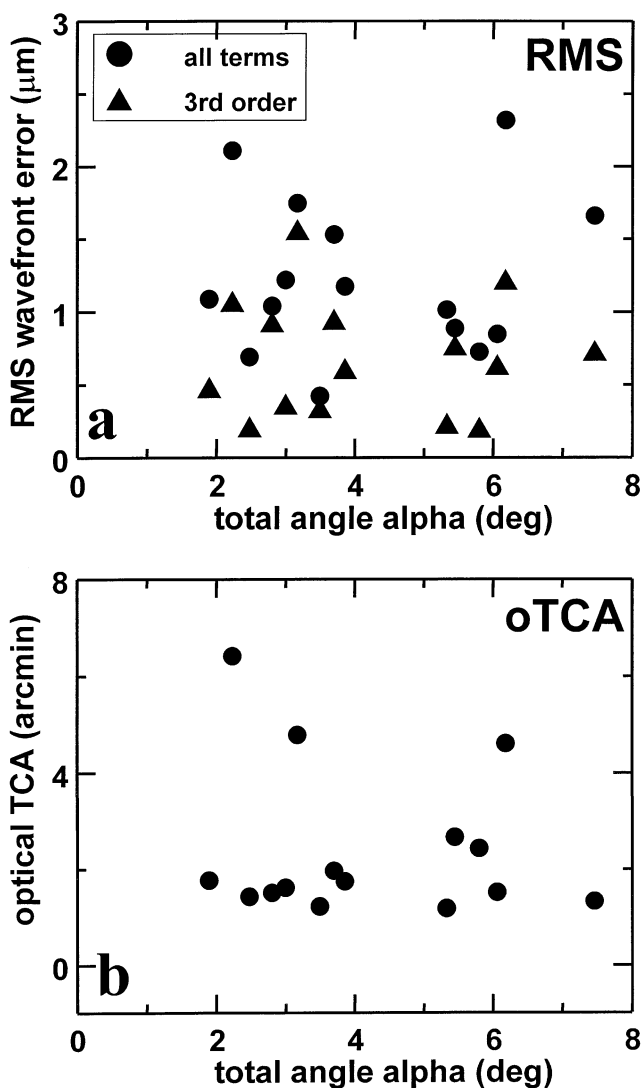


Fig. 6. (a) RMS wavefront error versus total angle alpha, for all terms (circles) and 3rd order terms (triangles), showing no correlation. (b) Optical transverse chromatic aberration versus total angle alpha, showing no correlation

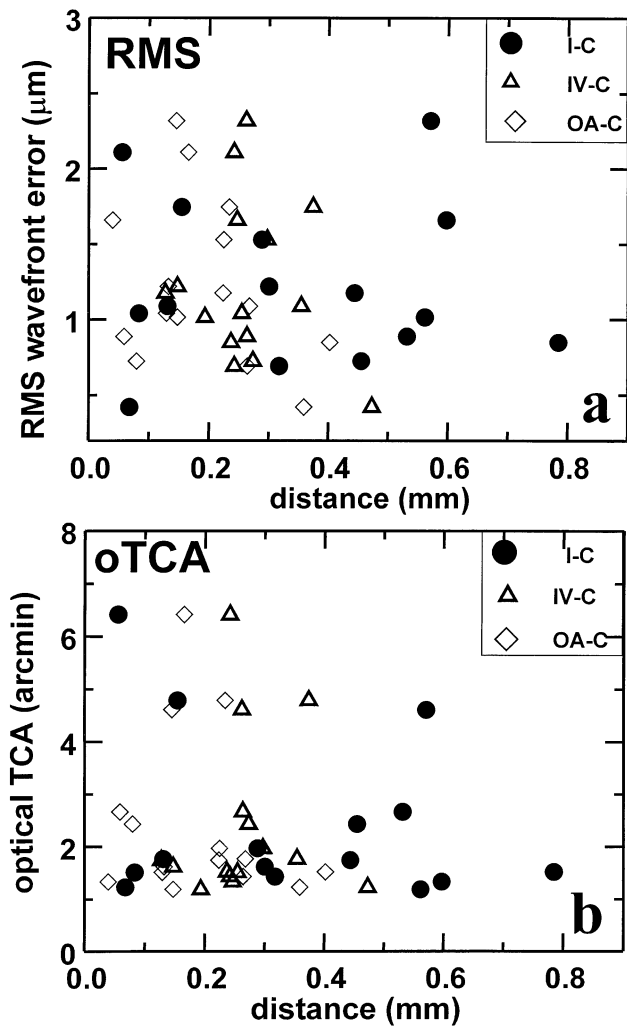


Fig. 7. (a) RMS wavefront error versus pupil centration—relative to 1st Purkinje image (I, solid circles), 4th Purkinje image (IV, open triangles) and optical axis (OA, open diamonds)—showing no correlation. (b) Optical TCA versus pupil centration—relative to 1st Purkinje image (solid circle), 4th Purkinje image (open triangle) and optical axis (open diamond)—showing no correlation.

of the 1st Purkinje image from the pupil center is represented with solid circles, the distance of the 4th Purkinje image from the pupil center is represented with open triangles, and the relative distance of the optical axis from the pupil center with open diamonds. We did not find any relationship between pupil centration (as measured relative to these three fixed positions) and ocular aberrations (both total and coma-like terms—not shown) or oTCA. Again, pupil centration (relative to 1st, 4th Purkinje images or optical axis) is symmetrical in left and right eyes of the same subject, whereas neither RMS nor oTCA is correlated in all left and right eyes of this group of subjects. This indicates that pupil decentration does not seem to be the major contributor to the variability found in the amount of aberrations and oTCA.

4.3. Hypothesis 3: corneal curvature and corneal asphericity

Corneal curvature and corneal asphericity contribute to the overall wave aberration, in particular to spherical aberration. One may argue that corneal curvature and corneal conicity may change the location of the nodal point. Using eye models, it can be calculated, if this displacement is sufficiently large, how it will affect the optical transverse chromatic aberration. We computed the RMS and oTCA for a four-surface wide-angle eye model (Escudero-Sanz & Navarro, 1999), as a function of curvature and conicity constant of the front surface of the cornea. Predictions were made for an angle alpha of +5 deg, and the pupil was assumed to be centered on the optical axis. Fig. 8(a) shows the predicted effect on RMS and oTCA for increasing corneal radii (from 7.4 to 8 mm), and for a conicity constant of $Q = -0.26$. The predicted RMS decreases slightly with corneal radius, whereas oTCA remains practically unchanged. We next computed that the nodal point displacement

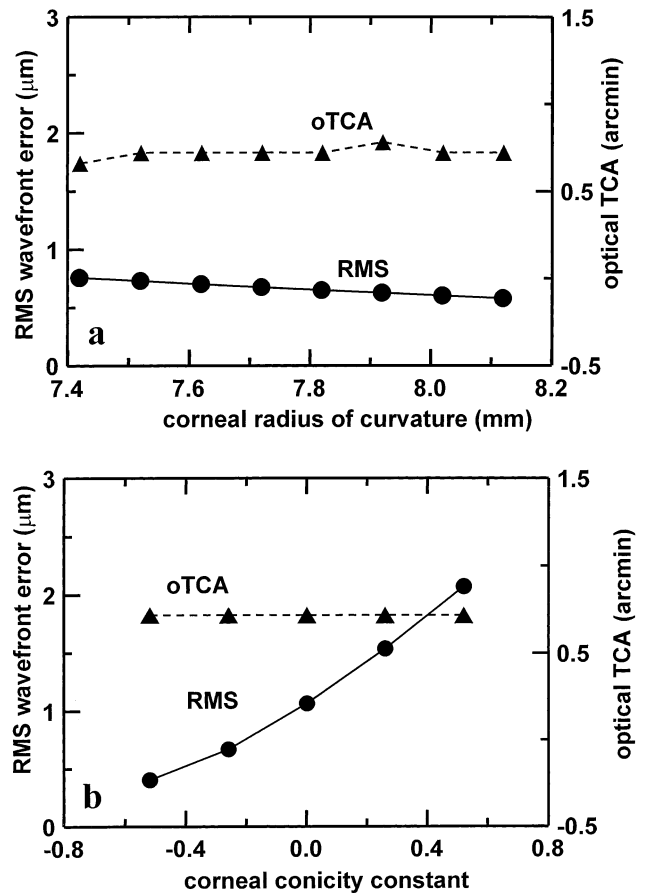


Fig. 8. Simulation (based on a four-surface wide-angle model) of the dependence of RMS wavefront error (circles, left y-axis) and optical TCA (triangles, right y-axis) on (a) corneal radius of curvature and (b) corneal conicity constant. RMS increases slightly with corneal radius and increases significantly with asphericity. Optical TCA is independent of these magnitudes.

produced by the change in corneal radius was 0.67 mm, equivalent to a change of only 0.06 deg, almost unnoticeable in terms of oTCA. Fig. 8(b) shows the predicted RMS and oTCA (for a fixed corneal radius of 7.72 mm) as corneal conicity constant increases: RMS increases (due to an increase in spherical aberration), whereas oTCA remains unchanged. Therefore, we conclude that the hypothesis that corneal conicity can explain the positive correlation of RMS and oTCA is not supported, since changes in corneal radius and corneal asphericity could not produce the common increase of RMS and oTCA.

4.4. Hypothesis 4: corneal irregularities

Besides tilt, misalignment, decentration and shape of optical components, irregularities in the optical components (cornea and lens) are expected to be major sources of aberrations. In our previous discussion, we have shown that variations in tilt, misalignment and decentration, or corneal shape do not appear to be common sources of increased monochromatic and optical chromatic aberrations in the tested eyes. By a process of elimination, either the shape of the crystalline lens or irregularities in the optical components could be major contributors. While the crystalline lens is not easily accessible in vivo, we did have data from a separate study that allowed us to evaluate the possible role of the cornea. The cornea is the major refracting surface of the eye, and it is well known that decreased corneal smoothness contributes substantially to increased wavefront aberrations of the human eye (Applegate, Howland, Sharp, Cottingham, & Yee, 1998; Oshika, Klyce, Applegate, Howland, & El Danasoury, 1999). We had corneal topography data available for six eyes in this study (S1, S4, and S5, right and left eyes). Corneal wavefront error was derived by applying standard ray tracing techniques to the corneal elevation maps, obtained with a Humphrey Instruments Atlas Corneal Topographer (Barbero, Marcos, Martín, Llorente, Moreno-Barriuso, & Merayo-Llves, 2001; Marcos, Barbero, Llorente, & Merayo-Llves, in press). Two of the eyes (S4-R and S5-R) were among those showing largest RMS and oTCA (see Figs. 2 and 3). Corneal RMS wavefront errors for these eyes (0.79 and 1.85 μm , respectively) were also higher than for the rest of measured eyes (average = 0.57 μm , standard deviation = 0.05 μm). Interestingly, subjects showing asymmetry between eyes in the overall ocular aberrations (S4 and S5) also had an asymmetry in the corneal aberrations. For subject S4, $\text{RMS}_{\text{right}}/\text{RMS}_{\text{left}} = 1.94$ for overall aberrations, and $\text{RMS}_{\text{right}}/\text{RMS}_{\text{left}} = 1.69$; for subject S5, $\text{RMS}_{\text{right}}/\text{RMS}_{\text{left}} = 4.14$ for overall aberrations, and $\text{RMS}_{\text{right}}/\text{RMS}_{\text{left}} = 2.98$ for corneal aberrations. This could explain the lack of correlation of aberrations between left and right eyes seen in Fig. 2,

which could not be explained by the previous hypotheses. It suggests that, at least in the most aberrated eyes of our study, corneal aberrations are a major contributor to the variability in monochromatic image quality.

Whereas corneal aberrations degrade image quality across the entire pupil, oTCA aberration is, by definition, measured locally at the pupil center. Conventional corneal topography data lack information on the central 1 mm of the cornea, and therefore simulations of oTCA using real corneal data are not possible. We have simulated the oTCA corresponding to the wide-angle model eye, with a smooth aspheric cornea, but with an irregularity (a spherical surface of 0.02 mm or a tilted plane) in the central cornea, and obtained oTCA values similar to those of the most aberrated eyes. This simulation indicates that it is possible that corneal imperfections in the central region cause an increase in oTCA. It is conceivable that these irregularities are more likely to happen in globally degraded corneas. Therefore, the correlation between RMS and oTCA found in Fig. 4 is not indicative of a correlation between a global measure (aberrations across the entire pupil) and a local measure (oTCA). Such correlation suggests that smooth corneas (providing good overall image quality, or low RMS) are not likely to exhibit central irregularities causing an increased oTCA, and alternatively, aberrated corneas (causing increased RMS) are likely to be degraded also centrally, causing an increase in oTCA. While data on the TCA at all pupil locations could test this model, the current data cannot reject the hypothesis that corneal irregularities account for a large proportion of the individual variation in RMS and oTCA.

The remaining possible sources for variations in optical quality are in the lens (optical properties, shape and irregularities) and the relative position of the cornea and lens. While the current study does not address these potential sources, it has rejected the most commonly cited sources for such variations in image quality.

5. Conclusions

1. There is a large inter-subject, and inter-eye variability in monochromatic aberrations and optical transverse chromatic aberration (oTCA). Eyes with a higher amount of monochromatic aberrations tend to have higher oTCA.
2. Tilt, misalignment of optical surfaces (front surface of the cornea and back surface of the lens) and the displacement of the fovea from the optical axis do not seem to be major contributors to the variation in monochromatic aberrations and oTCA.

3. Pupil decentration does not appear to be correlated to RMS wavefront error or oTCA.
4. Simulations show that corneal curvature and corneal asphericity alone cannot explain the relation between increased RMS and increased oTCA.
5. Corneal aberrations may play an important role in determining the overall image quality. Irregularities in the central corneal region are speculated to be a possible source of oTCA.

Acknowledgements

The authors acknowledge support by National Institutes of Health Grant EYO4395 to S.A. Burns, Human Frontier Science Programs HFSP LT0542/1997-B to S. Marcos and LT0326/1999-B to P.M. Prieto, Comisión Interministerial de Ciencia y Tecnología TIC98-0925-C02-01 to R. Navarro and CSIC Fellowship to B. Baraibar. We thank Carl Zeiss, S.A. Madrid for loan of a Humphrey Instrument Corneal Topography system, R. Scharf from Humphrey Instruments for help with the interface software and Sergio Barbero for corneal topography data analysis. We also thank J.S. McLellan for helpful discussions.

References

- Applegate, R. A., & Howland, H. C. (1997). Refractive surgery, optical aberrations, and visual performance. *Journal of Refractive Surgery*, *13*, 295–299.
- Applegate, R. A., Howland, H. C., Sharp, R. P., Cottingham, A. J., & Yee, R. W. (1998). Corneal aberrations and visual performance after radial keratotomy. *Journal of Refractive Surgery*, *14*, 397–407.
- Artal, P., Marcos, S., Iglesias, I., & Green, D. G. (1996). Optical modulation transfer function and contrast sensitivity with decentered small pupils. *Vision Research*, *6*, 3575–3586.
- Atchison, D. A., & Smith, G. (2000a). Axes of the eye. In *Optics of the human eye* (pp. 30–38). Oxford: Butterworth-Heinemann.
- Atchison, D. A., & Smith, G. (2000b). Monochromatic aberrations of schematic eyes. In *Optics of the human eye*. Oxford: Butterworth-Heinemann.
- Barbero, S., Marcos, S., Martín, R., Llorente, L., Moreno-Barriuso, E., & Merayo-Llodes, J. M. (2001). Validating the calculation of corneal aberrations from corneal topography: a test on keratoconus and aphakic eyes. *Investigative Ophthalmology and Visual Science (Supplement)*, *42*, 197.
- Barry, J. C., Effert, R., Kaupp, A., & Burhoff, A. (1994). Measurement of ocular alignment with photographic Purkinje I and IV reflection pattern evaluation. *Investigative Ophthalmology and Visual Science*, *35*, 4219–4235.
- Bennett, A. G., & Rabbetts, R. B. (1984). *Clinical visual optics* (first ed.). London: Butterworths.
- Bradley, A., Thibos, L., Zhang, X. X., Ye, M. (1991). The effects of ocular chromatic aberration on visual performance for displayed achromatic and chromatic information. Paper presented at the Society for Information Display International Symposium, Anaheim, CA.
- Burns, S. A., & Marcos, S. (2001). Measurement of the image quality of the eye with the spatially resolved refractometer. In S. MacRea, R. Krueger, & R. Applegate, *Customized corneal ablations*. Thorofare, NJ: Slack.
- Campbell, M. W., Haman, H., Simonet, P., & Brunette, I. (1999). Dependence of optical image quality on refractive error: eyes after excimer laser photorefractive keratectomy (PRK) versus controls. *Investigative Ophthalmology and Visual Science (Supplement)*, *40*, 7.
- Charman, W. N. (1991). Wavefront aberrations of the eye: a review. *Optometry and Vision Science*, *68*, 574–583.
- Charman, W. N., & Jennings, J. A. M. (1976). Objective measurements of the longitudinal chromatic aberration of the human eye. *Vision Research*, *16*, 999–1005.
- Cornsweet, T. N., & Crane, H. D. (1973). Accurate two-dimensional eye tracker using first and fourth Purkinje images. *Journal of the Optical Society of America A*, *63*, 921–928.
- Dunne, M. C. M., Barry, J. C., Hartmann, A., Culpin, F., de Main, J., & French, I. (1995). Measurement of the corneal and crystalline lens misalignment relative to the visual axis. *Vision Research (Supplement)*, *35*, 199.
- Escudero-Sanz, I., & Navarro, R. (1999). Off-axis aberrations of a wide-angle schematic eye model. *Journal of the Optical Society of America A*, *16*, 1–11.
- He, J. C., Burns, S. A., & Marcos, S. (2000). Monochromatic aberrations in the accommodated human eye. *Vision Research*, *40*, 41–48.
- He, J. C., Marcos, S., Webb, R. H., & Burns, S. A. (1998). Measurement of the wave-front aberration of the eye by a fast psychophysical procedure. *Journal of the Optical Society of America A*, *15*, 2449–2456.
- Howarth, P. A., & Bradley, A. (1986). The longitudinal chromatic aberration of the human eye, and its correction. *Vision Research*, *26*, 361–366.
- Howland, B., & Howland, H. C. (1976). Subjective measurement of high-order aberrations of the eye. *Science*, *193*, 580–582.
- Howland, H. C., & Howland, B. (1977). A subjective method for the measurement of the monochromatic aberrations of the eye. *Journal of the Optical Society of America A*, *67*, 1508–1518.
- Iglesias, I., Berrio, E., & Artal, P. (1998). Estimates of the ocular wave aberration from pairs of double-pass retinal images. *Journal of the Optical Society of America A*, *15*, 2466–2476.
- Le Grand, Y., & El Hage, S. G. (1980). *Physiological optics*, vol. 1. Berlin: Springer.
- Liang, J., Grimm, B., Goelz, S., & Bille, J. F. (1994). Objective measurement of wave aberrations of the human eye with the use of a Hartmann–Shack wave-front sensor. *Journal of the Optical Society of America A*, *11*, 1949–1957.
- Liang, J., & Williams, D. R. (1997). Aberrations and retinal image quality of the normal human eye. *Journal of the Optical Society of America A*, *14*, 2873–2883.
- Liang, J., Williams, D. R., & Miller, D. T. (1997). Supernormal vision and high resolution retinal imaging through adaptive optics. *Journal of the Optical Society of America A*, *14*, 2884–2892.
- Liou, H.-L., & Brennan, N. A. (1997). Anatomically accurate, finite model eye for optical modelling. *Journal of the Optical Society of America A*, *14*, 1684–1695.
- Lotmar, W. (1971). Theoretical eye model with aspheric surfaces. *Journal of the Optical Society of America A*, *61*, 1522–1529.
- Marcos, S., Barbero, S., Llorente, L., & Merayo-Llodes, J. (in press). Optical response to myopic LASIK surgery from total and corneal alterations. *Investigative Ophthalmology and Visual Science*.
- Marcos, S., & Burns, S. A. (2000). On the symmetry between eyes of wavefront aberration and cone directionality. *Vision Research*, *40*, 2437–2447.

- Marcos, S., Burns, S. A., Moreno-Barriuso, E., & Navarro, R. (1999). A new approach to the study of ocular chromatic aberrations. *Vision Research*, *39*, 4309–4323.
- Moreno-Barriuso, E., Merayo-Llodes, J. M., Marcos, S., Llorente, L., Navarro, R., & Barbero, S. (2001). Ocular aberrations before and after refractive surgery: LASIK-induced changes measured with laser ray tracing. *Investigative Ophthalmology and Visual Science*, *42*, 1396–1403.
- Navarro, R., & Losada, M. A. (1997). Aberrations and relative efficiency of light pencils in the living human eye. *Optometry and Vision Science*, *74*, 540–547.
- Navarro, R., Moreno-Barriuso, E., Bará, S., & Mancebo, T. (2000). Phase-plates for wave-aberration compensation in the human eye. *Optics Letters*, *25*, 236–238.
- Navarro, R., Santamaria, J., & Bescós, J. (1985). Accommodation-dependent model of the human eye with aspherics. *Journal of the Optical Society of America A*, *2*, 1273–1281.
- Ogobso, Y. U., & Bedell, H. E. (1987). Magnitude of lateral chromatic aberration across the retina of the human eye. *Journal of the Optical Society of America A*, *4*, 1666–1672.
- Oshika, T., Klyce, S. D., Applegate, R. A., Howland, H. C., & El Danasoury, M. A. (1999). Comparison of corneal wavefront aberrations after photorefractive keratectomy and laser in situ keratomileusis. *American Journal of Ophthalmology*, *127*, 1–7.
- Phillips, P., Perez-Emmanuelli, J., Rosskothén, H. D., & Koester, C. J. (1988). Measurement of intraocular lens decentration and tilt in vivo. *Journal of Cataract and Refractive Surgery*, *14*, 129–135.
- Rynders, M. C., Lidkea, B. A., Chisholm, W. J., & Thibos, L. N. (1995). Statistical distribution of foveal transverse chromatic aberration, pupil centration and angle ψ in a population of young adult eyes. *Journal of the Optical Society of America A*, *12*, 2348–2357.
- Rynders, M. C., Navarro, R., & Losada, M. A. (1998). Objective measurement of the off-axis longitudinal chromatic aberration in the human eye. *Vision Research*, *38*, 513–522.
- Seiler, T., Kaemmerer, M., Mierdel, P., & Krinke, H.-E. (2000). Ocular optical aberrations after photorefractive keratectomy for myopia and myopic astigmatism. *Archives of Ophthalmology*, *118*, 17–21.
- Simonet, P., & Campbell, M. C. W. (1990). The optical transverse chromatic aberration on the fovea of the human eye. *Vision Research*, *30*(2), 187–206.
- Thibos, L. N. (1987). Calculation of the influence of lateral chromatic aberration on image quality across the visual field. *Journal of the Optical Society of America A*, *4*, 1673–1680.
- Thibos, L. N., Applegate, R. A., Schwiegerling, J. T., Webb, R. H., & Members, V. S. T. (2000). Standards for reporting the optical aberrations of eyes. In *Vision science and its applications trends in optics and photonics*, vol. 35. Santa Fe, NM: Optical Society of America.
- Thibos, L. N., Bradley, A., Still, D. L., Zhang, X., & Howarth, P. A. (1990). Theory and measurement of ocular chromatic aberration. *Vision Research*, *30*, 33–49.
- Thibos, L. N., Ye, M., Zhang, X. X., & Bradley, A. B. (1992). The chromatic eye: a new reduced-eye model of ocular chromatic aberration in humans. *Applied Optics*, *31*, 3594–3600.
- Tscherning, M. (1924). *Physiological optics*. Philadelphia, PA: Keystone.
- Van Meeteren, A. (1974). Calculations on the optical modulation transfer function of the human eye for white light. *Optica Acta*, *21*, 395–412.
- Van Meeteren, A., & Dunnewold, C. J. W. (1983). Image quality of the human eye for eccentric pupils. *Vision Research*, *23*, 573–579.
- Vargas-Martin, F., Prieto, P. M., & Artal, P. (1998). Correction of the aberrations in the human eye with a liquid-crystal spatial light modulator: limits to performance. *Journal of the Optical Society of America A*, *15*, 2552–2562.
- Walsh, G. (1988). The effect of mydriasis on the pupillary centration of the human eye. *Ophthalmology and Physiology Optics*, *8*, 178–182.
- Walsh, G., & Charman, W. N. (1988). The effect of pupil centration and diameter on ocular performance. *Vision Research*, *28*, 659–665.
- Webb, R. H., Penney, C. M., & Thompson, K. P. (1992). Measurement of ocular wavefront distortion with a spatially resolved refractometer. *Applied Optics*, *31*, 3678–3686.
- Wilson, M. A., Campbell, M. C. W., & Simonet, P. (1992). Change of pupil centration with change of illumination and pupil size. *Optometry and Vision Science*, *69*, 129–136.
- Zhu, L., Sun, P., Bartsch, D., Freeman, W. R., & Fainman, Y. (1999). Adaptive control of a micromachined continuous-membrane deformable mirror for aberration compensation. *Applied Optics*, *38*, 168–176.